Modeling of a viscous fluid percolating a porous material due to capillary forces

Johannesson, Björn

2000

LUND INSTITUTE OF TECHNOLOGY
LUND UNIVERSITY

Division of Building Materials

Modeling of a Viscous Fluid Percolating a Porous Material due to Capillary Forces

Björn Johannesson

TVBM-3095 Lund 2000

LUND INSTITUTE OF TECHNOLOGY
LUND UNIVERSITY

Division of Building Materials

Modeling of a Viscous Fluid Percolating a Porous Material due to Capillary Forces

Björn Johannesson

TVBM-3095 Lund 2000

ISRN LUTVDG/TVBM--00/3095--SE(1-24)
ISSN 0348-7911 TVBM

Lund Institute of Technology
Division of Building Materials
Box 118
SE-221 00 Lund, Sweden

Telephone: 46-46-2227415
Telefax: 46-46-2224427
www.byggnadsmaterial.lth.se

Modeling of a Viscous Fluid Percolating a Porous Material due to Capillary Forces

Björn F. Johannesson
Division of Building Materials, Lund Institute of Technology
Box 118, SE-221 00 Lund, Sweden

Abstract

Percolation of a fluid into a porous material is modeled by using a mixture theory defined within modern continuum mechanics. The phenomenon referred to as capillary suction has many negative effects on materials used in building constructions. For example, the mass concentration of liquid water and its percolation velocity in a porous material, such as concrete, are essential factors when the dissolved ion concentrations within the pore solution are of interest. Other examples are the swelling of the porous material due to the presence of capillary water eventually contributing to cracks in the material. A model in which the velocity and the mass density in the percolating fluid, and the stress in the solid can be calculated is developed. Two test examples are solved using the finite element method. There is good agreement between experimental observations on less dense materials, such as concrete and sandstones, and the simulations performed.

1 Introduction

The capillary suction of fluids in porous materials is most often treated as a potential flow. The governed equation to be solved is then Fick's second law with a strong non-linearity of the parameter relating the mass density flow to the gradient of the mass density. Here another approach is studied, namely, a compressible viscous fluid which is percolating the pore structure due to differences between the stress in the outer fluid and the fluid present within the material. The fluid is assumed to be subjected to loss of momentum

due to the 'friction' forces induced by the liquid-pore wall interfaces. This momentum loss is constituted to be proportional to the difference between the fluid velocity and the velocity of the solid in which the fluid is sucked.

The assumed symmetric partial stress tensors for the fluid and the solid are constituted in a classical fashion. The Navier-Poisson law of a Newtonian fluid is assumed and a linear elastic solid with assumed small displacements and rigid-rotations is adopted. The thermodynamic equilibrium pressure in the fluid (which is independent of the velocity gradient) is assumed to depend on the mass density of the same fluid in a given pore structure, i.e. the pore structure is characterized in terms of the pore-size distribution assuming straight cylindrical pores together with an assumption of the wetting angle between the liquid-air interface and the solid pore wall interface. That is, the concept of capillary pressure based on the so-called Laplace formula, e.g. compare [1], can be used. The partial stress in the solid is also assumed to be dependent on the mass density of the fluid within the pore structure from a fixed state where no swelling exists.

The strategy is, loosely speaking, to solve the momentum balance equation and the constitutive equations for the fluid in terms of the velocity fields. The 'known' velocity field of the fluid together with the mass balance equation can then be used to calculate the mass density for the same fluid without specifying any new constitutive equations, i.e. no mass exchanges between the fluid and the solid are considered. The 'known' velocity field and mass density of the fluid can, further, be used to calculate the displacements in the solid by using the momentum balance and constitutive equations related to the solid. Obviously, a quite complex equation system has to be solved compared to the standard potential flow equations often adopted to model capillary suction. However, it is my belief that results from simulation using different theories and strategies can contribute to an increase in our knowledge of real physical phenomena taking place. Therefore this more complex equation system will be established and solved. The results are compared to measured responses found in concrete specimens subjected to water uptake.

The mixture theory described in [2] will be used to develop the model. It should be noted, however, that more detailed mixture theory approaches have been developed recently. One of them is the hybrid mixture theory which is a combination of 'classical' mixture theory (described at macroscale) and averaging of microscale balance equations, e.g. see [3] and [4]. Another similar approach based on hybrid mixture theory has also been developed where balance equations are also postulated for interfaces between different phases

in a mixture [5]. This approach has been used to model swelling and shrinking systems where interactions between various phases play a significant role. It is believed that the capillary suction phenomenon is a problem where the behavior of the interfaces of the liquid and the solid is crucial. Here, however, the mixture theory as described by Bowen [2] will be used, which is a theory developed at macroscale without any explicit considerations of microscale and interfaces between different phases. Therefore the effect of the physical behavior at microscale and mesoscale and the effect of interfaces at these scales must rather be incorporated in the introduced material coefficients directly at the macroscale.

It will be shown that the experimentally verified (global) response in terms of capillary suction of water into materials such as less dense concretes and sandstones can be obtained by using the model to be presented. One problem related to the model is that a quite complex non-linear equation system must be dealt with. Further, some uncertainties concerning the choice of physically sound boundary conditions in the momentum equation describing the percolating fluid must be dealt with.

Percolation velocities and moisture content due to capillary suction of water into porous materials, such as concrete, are factors related to the determination of the service life of surfaces in outdoor building constructions. Such issues are discussed in [6].

2 Mass and Momentum Balance for individual constituents in a mixture

In this section the mixture theory as described in [2] will be used. Far from all aspects of this theory will be discussed in this work. The main strategies on which the mixture theory is developed may, however, be of importance. The mixture theory rests on three so-called metaphysical principles as described by Truesdell, e.g. compare [7]. These principles are, *(i)* all properties of the mixture must be mathematical consequences of properties of the constituent. *(ii)* in order to describe the motion of a constituent, we may in imagination isolate it from the rest of the mixture, provided we allow properly for actions of the other constituents upon it, *(iii)* the motion of the mixture is governed by the same equations as is a single body.

Mass balance for an individual constituent present in a mixture may be

formulated in local form as, e.g. compare [2],

$$\frac{\partial \rho_a}{\partial t} = -\mathrm{div}\left(\rho_a \mathbf{x}_a^{'}\right) + \hat{c}_a; \qquad a = 1, ..., \Re, \tag{1}$$

where $\rho_a(\mathbf{x}, t)$ is the mass density of an arbitrary constituent denoted a. The total number of constituents is denoted $\Re$. The velocity of the a:th constituent is denoted $\mathbf{x}_a^{'}(\mathbf{x}, t)$ and $\hat{c}_a$ denotes the mass exchange rate to the a:th constituent from all other constituents present in the mixture. Due to the mass balance for the whole mixture one must assure that there is no net production of mass in a material point, i.e. $\sum_{a=1}^{\Re} \hat{c}_a(\mathbf{x}, t) = 0$. The derivative $\partial \rho_a / \partial t$ denotes the spatial time derivative of the mass density of the a:th constituent.

In the capillary suction problem to be studied, no mass exchanges will be considered. That is, the equation (1) simplifies to

$$\frac{\partial \rho_a}{\partial t} = -\mathrm{div}\left(\rho_a \mathbf{x}_a^{'}\right); \qquad a = 1, ..., \Re, \tag{2}$$

The mass balance for the whole mixture in local form is the postulate

$$\frac{\partial \rho}{\partial t} = -\mathrm{div}\left(\rho \dot{\mathbf{x}}\right) \tag{3}$$

where $\dot{\mathbf{x}}$ is the mean velocity or simply the velocity of the mixture and ρ is the mass density of the mixture. The mean velocity is defined as $\dot{\mathbf{x}}(\mathbf{x}, t) = \frac{1}{\rho} \sum_{a=1}^{\Re} \rho_a \mathbf{x}_a^{'}(\mathbf{x}, t)$ and the mass density of the mixture is defined as $\rho(\mathbf{x}, t) = \sum_{a=1}^{\Re} \rho_a(\mathbf{x}, t)$.

The momentum balance for the a:th constituent in local form is the postulate

$$\rho_a \frac{\partial \mathbf{x}_a^{'}}{\partial t} + \rho_a \left[\mathrm{grad}\, \mathbf{x}_a^{'}\right] \mathbf{x}_a^{'} = \mathrm{div}\, \mathbf{T}_a + \rho_a \mathbf{b}_a + \hat{\mathbf{p}}_a; \qquad a = 1, ..., \Re, \tag{4}$$

where $\partial \mathbf{x}_a^{'} / \partial t$ denotes the spatial time derivative of the velocity $\mathbf{x}_a^{'}$. The stress tensor for the a:th constituent is denoted $\mathbf{T}_a$ and $\mathbf{b}_a$ denotes the body force density. The term $\hat{\mathbf{p}}_a$ represents the so-called momentum supply which models the interaction of thermodynamic forces among the constituents. The stress tensor $\mathbf{T}_a$ is indeed allowed to be non-symmetric when adopting the mixture theory as described by for example [2]; here, however, it will be explicitly assumed that $\mathbf{T}_a$ is symmetric, i.e. $\mathbf{T}_a - \mathbf{T}_a^{\mathrm{T}} = \mathbf{0}$. In order to assure

that a summation of the equation (4), for all $\Re$ constituents, is identical to the momentum balance for the whole mixture one must assure that $\sum_{a=1}^{\Re} \hat{\mathbf{p}}_a = \mathbf{0}$, which is the proper condition for the mixture in situations when no mass exchanges between constituents are considered.

The momentum balance, in local form, for the whole mixture is the postulate

$$\rho \frac{\partial \dot{\mathbf{x}}}{\partial t} + \rho \left[\operatorname{grad} \dot{\mathbf{x}}\right] \dot{\mathbf{x}} = \operatorname{div} \mathbf{T} + \rho \mathbf{b} \tag{5}$$

The total stress tensor for the whole mixture is denoted $\mathbf{T}$ and is defined as $\mathbf{T}(\mathbf{x}, t) = \sum_{a=1}^{\Re} (\mathbf{T}_a + \rho_a \mathbf{u}_a \otimes \mathbf{u}_a)$ where $\mathbf{u}_a$ is the diffusion velocity of the a:th constituent. The diffusion velocity $\mathbf{u}_a$ is defined as $\mathbf{u}_a(\mathbf{x}, t) = \mathbf{x}_a'(\mathbf{x}, t) - \dot{\mathbf{x}}(\mathbf{x}, t)$, i.e. $\mathbf{u}_a$ is the velocity for the a:th constituent related to the velocity of the mixture $\dot{\mathbf{x}}$. The somewhat complex definition of the total stress tensor $\mathbf{T}$ is a direct consequence of requiring the momentum balance for the individual constituents, i.e. equation (4) to be compatible with the postulated momentum balance for the whole mixture, i.e. equation (5). The body force vector $\mathbf{b}$ is simply defined as the mass weighted sum of the individual body force vectors, i.e. $\mathbf{b}(\mathbf{x}, t) = \frac{1}{\rho} \sum_{a=1}^{\Re} \rho_a \mathbf{b}_a(\mathbf{x}, t)$.

3 Constitutive relations for the capillary suction problem

The general concepts for developing constitutive relations will be used to model the problem of capillary suction of a viscous fluid into a porous material. These general concepts consist of restrictions imposed by the second axiom of thermodynamics, restrictions imposed by the axiom of material frame-indifference and finally the restrictions imposed by material symmetry. In this case only isotropic material functions will be studied. The concepts from the second axiom of thermodynamics will only be utilized to confirm the generalization of the Stokes relation, i.e. the relation between the volumetric viscosity and the shear viscosity. This relation assures that the dissipation due to the appearance of the stress power in the fluid is always a non-negative quantity, i.e. $\operatorname{tr}(\mathbf{T}_f \mathbf{D}_f) \geq 0$. The combined effect of material frame-indifference and isotropic material functions means, further, that the stress tensor for the assumed isotropic solid and the assumed isotropic fluid

are described with two material parameters only, i.e. the so-called Lame's parameters. Furthermore, the axiom of material frame-indifference can be used to show that the momentum supply cannot depend on the velocity. However, by the same axiom it can be proven that velocity differences among different constituents (in this case the velocity difference between the fluid and the solid material) can be used to relate constitutive dependent and independent properties and still satisfy the frame-indifference axiom, compare [2].

The 10 introduced constitutive independent properties in the studied capillary suction problem are

$$\begin{array}{ll} \mathbf{x}_f'(\mathbf{x},t)\,; & \mathbf{x}_s'(\mathbf{x},t) \approx \mathbf{0} \\ \rho_f(\mathbf{x},t)\,; & \rho_s(\mathbf{x},t) \approx \text{const.} \\ \dot{\mathbf{x}}(\mathbf{x},t)\,; & \mathbf{w}_s(\mathbf{x},t) \end{array} \tag{6}$$

where $\mathbf{x}_f'$ and $\mathbf{x}_s'$ are the velocity of fluid and solid respectively. The mass density concentrations of the same two constituents are denoted by ρ_f and ρ_s, $\dot{\mathbf{x}}$ is the velocity of the mixture, and $\mathbf{w}_s$ is the displacement vector of the solid.

The 25 introduced constitutive dependent properties are the mechanical properties

$$\begin{array}{ll} \mathbf{T}_f^n(\mathbf{x},t)\,; & \mathbf{T}_s(\mathbf{x},t) \\ \hat{\mathbf{p}}_f(\mathbf{x},t)\,; & \hat{\mathbf{p}}_s(\mathbf{x},t) \\ \pi_f^e(\mathbf{x},t) & \end{array} \tag{7}$$

where $\mathbf{T}_f^n$ and $\mathbf{T}_s$ are the non-equilibrium part of the stress in the fluid (i.e. stresses due to velocity gradients only) and the stress tensor for the solid, respectively. The properties $\hat{\mathbf{p}}_f$ and $\hat{\mathbf{p}}_s$ denote the corresponding momentum supplies of the two constituents, and π_f^e is the equilibrium thermodynamic pressure in the fluid. In other words, a total of 35 unknowns are searched for in this specific model.

The constitutive dependent properties in (7) are assumed to be related to the constitutive independent properties in (6), by the following general format

$$\left(\mathbf{T}_f^n, \pi_f^e, \mathbf{T}_s, \hat{\mathbf{p}}_f, \hat{\mathbf{p}}_s\right) = \mathbf{f}\left(\operatorname{grad}\mathbf{x}_f', \operatorname{grad}\mathbf{w}_s, \operatorname{grad}\rho_f, \mathbf{x}_f' - \mathbf{x}_s', \rho_f\right) \tag{8}$$

There are 6 momentum balance equations for the fluid and 6 momentum balance equations for the solid when assuming symmetric partial stress tensors. From the mixture theory one also has 3 equations for the momentum

supplies, i.e. $\hat{\mathbf{p}}_f = -\hat{\mathbf{p}}_s$. Finally, one mass balance equation is introduced. That is, in total 16 balance equations are available. That is, $35 - 16 = 19$ constitutive relations are required. Assuming, further that $\mathbf{x}_s^{'}(\mathbf{x},t) \approx \mathbf{0}$ the definition $\dot{\mathbf{x}}(\mathbf{x},t) = \frac{1}{\rho}\sum_{a=1}^{2}\rho_a \mathbf{x}_a^{'}(\mathbf{x},t)$ gives that $\dot{\mathbf{x}}(\mathbf{x},t) \approx \frac{\rho_a}{\rho}\mathbf{x}_f^{'}(\mathbf{x},t)$ which reduces the required number of constitutive relations to 16.

Assuming the partial stress tensor $\mathbf{T}_f$ for the fluid percolating the pore structure to be symmetric and to be dependent on the symmetric part of the velocity gradient $\mathbf{D}_f = \frac{1}{2}(\operatorname{grad}\mathbf{x}_f^{'} + \left(\operatorname{grad}\mathbf{x}_f^{'}\right)^{\mathrm{T}})$ and on the thermodynamic pressure π_f^e, the constitutive relation for the 6 stress components must be of the form

$$\mathbf{T}_f = -\pi_f^e\mathbf{I} + \lambda_f(\operatorname{tr}\mathbf{D}_f) + 2\mu_f\mathbf{D}_f \tag{9}$$

which follows from the requirement of objectivity for symmetric tensor functions. The material parameters λ_f and μ_f represent the volumetric viscosity and shear viscosity of the fluid, respectively. Due to the second axiom of thermodynamics λ_f and μ_f must be related as

$$\lambda_f \geq -\tfrac{2}{3}\mu_f \qquad \text{and} \qquad \mu_f \geq 0 \tag{10}$$

which is a generalization of the Stoke's relation, i.e. $\lambda_f = -\frac{2}{3}\mu_f$.

The equilibrium pressure π_f is a thermodynamic pressure which can be a function of the mass density of the fluid present in the material and a function of $\operatorname{tr}(\mathbf{E}_s)$, where $\mathbf{E}_s$, see equation (14), is the strain tensor. The term $\operatorname{tr}(\mathbf{E}_s)$ is an invariant measure representing the volume of the solid with respect to a reference volume. The following constitutive assumption is used for π_f:

$$\pi_f^e = \kappa_{fs}\rho_f + \gamma_{fs}\operatorname{tr}(\mathbf{E}_s) \tag{11}$$

By assuming κ_{fs} to be a function of the pore distribution curve, for a certain material, the stress in the fluid, induced by curved water-air interfaces, can be introduced as a smeared pressure directly on the macro-scale. The inclusion of the second term on the right-hand side of (11) is due to the effect of the strain in the solid changing the Kelvin radius, i.e. the curved water-air interface is changed when the solid is strained.

The momentum supply between the fluid and the porous material is the constitutive relation for the three supply components

$$\hat{\mathbf{p}}_f = -\xi_{fs}\left(\mathbf{x}_f^{'} - \mathbf{x}_s^{'}\right) - \vartheta_{fs}\operatorname{grad}\rho_f \tag{12}$$

where ξ_{fs} represents a material parameter which relates the momentum supply for the fluid to the velocity of the fluid relative to the velocity of the solid. The first term on the right-hand side of (12) is often referred to as the Stokes drag formula. The inclusion of the second term $\vartheta_{fs}\text{grad}\rho_f$ can be argued for by imagining a body submerged in a fluid. The body will experience a force proportional to the density difference between the body and the fluid. The physical argument is that in the limit of a large number of submerged bodies this force is proportional to the density gradients of the constituents in the resulting mixture. The term $\vartheta_{fs}\text{grad}\rho_f$ in (12) can, therefore, be referred to as a buoyancy force, although this force has nothing to do with the absence or presence of a gravitational force.

The 6 stress components for the solid porous material are assumed given by the constitutive function

$$\mathbf{T}_s = \lambda_s \left(\text{tr}\mathbf{E}_s\right)\mathbf{I} + 2\mu_s\mathbf{E}_s - \tau_s\left(\rho_f - \rho_f^+\right)\mathbf{I} \tag{13}$$

where $\mathbf{E}_s$ is the linear strain measure for the solid valid for situations with small displacement gradients and small rigid body rotations, i.e.

$$\mathbf{E}_s = \frac{1}{2}\left(\text{GRAD}\,\mathbf{w}_s + \left(\text{GRAD}\,\mathbf{w}_s\right)^{\text{T}}\right) \tag{14}$$

where $\mathbf{w}_s = \mathbf{w}_s\left(\mathbf{X}_s, t\right) = \boldsymbol{\chi}_s\left(\mathbf{X}_s, t\right) - \mathbf{X}_s$ is the displacement of the solid. The current place $\mathbf{x}$ is given by the deformation function $\boldsymbol{\chi}_s$ as $\boldsymbol{\chi}_s\left(\mathbf{X}_s, t\right) = \mathbf{x}$ and $\mathbf{X}_s$ represents the initial configuration of the solid. The operator GRAD denotes the gradient with respect to the initial configuration $\mathbf{X}_s$.

Finally, it is noticed that the equation system is closed since the 16 required constitutive relations are introduced. That is 6 constitutive relations for the solid stress components and fluid stress components, respectively, and one constitutive equation for the thermodynamic equilibrium pressure, and 3 equations for the momentum supply components.

4 Governing equations

The momentum balance for the fluid, compare equation (4), and the constitutive relation for the partial stress tensor $\mathbf{T}_f$, i.e. (9) where the volumetric viscosity $\lambda_f = 0$, and the constitutive relation (12) for the momentum supply

$\hat{\mathbf{p}}_f$ combine to yield

$$\begin{aligned}\rho_f \frac{\partial \mathbf{x}_f^{'}}{\partial t} &= -\rho_f \left[\operatorname{grad} \mathbf{x}_f^{'}\right] \mathbf{x}_f^{'} \\ &+\operatorname{div}\left(-\left(\kappa_{fs}\rho_f + \gamma_{fs}\operatorname{tr}\left(\mathbf{E}_s\right)\right)\mathbf{I} + 2\mu_f \mathbf{D}_f\right) \\ &+\rho_f \mathbf{b}_f - \xi_{fs}\left(\mathbf{x}_f^{'} - \mathbf{x}_s^{'}\right) - \vartheta_{fs}\operatorname{grad}\rho_f\end{aligned} \tag{15}$$

where the assumption for the thermodynamic pressure has been inserted, i.e.

$$\pi_f^e = \kappa_{fs}\rho_f + \gamma_{fs}\operatorname{tr}\left(\mathbf{E}_s\right) \tag{16}$$

which is equation (11) repeated. The argument for setting $\lambda_f = 0$ when the fluid constituent has a symmetric stress and no mass exchanges with other constituents will be explained in the following. The mass balance for the fluid in the conditions described above, i.e. $\mathbf{T}_f = \mathbf{T}_f^{\mathrm{T}}$ and $\hat{c}_f = 0$, can be expressed as $\operatorname{tr}\mathbf{D}_f = -\rho_f^{'}/\rho_f$, where $\rho_f^{'}$ is the material time derivative following the motion of the fluid constituent. The value of $\rho_f^{'}$ is in this model allowed to deviate significantly from zero, making also $\operatorname{tr}\mathbf{D}_f \neq 0$. The value of $\operatorname{tr}\mathbf{D}_f$ will, however, be assumed not to contribute to any stresses in the fluid. This is the argument for setting the volumetric viscosity λ_f equal to zero and still allowing for the mass density of the fluid in a representative volume of the solid to be changed during the capillary suction process.

The momentum balance equation for the solid, e.g. compare (4), combined with the equations (12) and (13) gives

$$\begin{aligned}\mathbf{0} &= \operatorname{div}\left(\lambda_s\left(\operatorname{tr}\mathbf{E}_s\right)\mathbf{I} + 2\mu_s\mathbf{E}_s - \tau_s\Delta\rho_f\mathbf{I}\right) + \rho_s\mathbf{b}_s \\ &+\xi_{fs}\left(\mathbf{x}_f^{'} - \mathbf{x}_s^{'}\right) + \vartheta_{fs}\operatorname{grad}\rho_f\end{aligned} \tag{17}$$

where $\rho_f - \rho_f^{+} = \Delta\rho_f$ and where $\hat{\mathbf{p}}_f = -\hat{\mathbf{p}}_s$ has also been used. In (17) the dynamic effects have been assumed to be negligible compared to the other terms.

The equation for determination of the mass density field $\rho_f\left(\mathbf{x}, t\right)$ of the fluid is simply the mass balance equation (3), i.e.

$$\frac{\partial \rho_f}{\partial t} = -\rho_f \operatorname{div}\mathbf{x}_f^{'} - \mathbf{x}_f^{'} \cdot \operatorname{grad}\rho_f \tag{18}$$

The boundary conditions to be used are not given by simple arguments in the studied capillary suction phenomena. The main problem is that the

thermodynamic pressure cannot be directly measured at the boundary. It is therefore difficult to argue for a certain choice of a value of a driving thermodynamic pressure at the boundary. It seems reasonable, however, to choose an essential boundary condition for the mass density of the fluid at the boundary surface exposed to capillary suction. This value should be the mass density of the fluid corresponding to a saturation of the pore space available for the capillary sucked fluid.

5 Finite element formulation in one dimension

In order to illustrate the solution behavior of the proposed equation system a numerical method must be adopted. Here a finite element formulation will be discussed. A one-step time integration scheme will be used as described in, for example, [8] and [9]. This time stepping scheme allows for both truly explicit and implicit integration in the time domain. Furthermore, standard weighting methods, such as the Crank-Nicholson scheme, can be used simply by specifying one parameter in the equation system.

Due to the 'convective' term $\rho_f \left[\text{grad}\, \mathbf{x}_f'\right] \mathbf{x}_f'$ in the equation describing the fluid constituent, i.e. equation (15), the standard Galerkin weighting method can give rise to important errors. Instead, the Petrov-Galarkin weighting will be adopted which has been developed by fitting a weighting parameter against analytical solutions to simple 'convective' one-dimensional problems. The mass balance equation will also be solved by using the Petrov-Galarkin weighting due to the presence of the term $\mathbf{x}_f' \cdot \text{grad}\, \rho_f$ which is interpreted as a 'convective' first-order derivative.

The equation system to be solved is coupled and non-linear. The non-linearity is mainly due to the 'convective' term $\rho_f \left[\text{grad}\, \mathbf{x}_f'\right] \mathbf{x}_f'$. Other types of non-linearities must of course be dealt with if, for example, the introduced material constants are assumed to be functions of the state variables such as the fluid mass density. Due to the somewhat complex structure of the transient equation system it is difficult to perform and find equilibrium solutions by iterations within each time step. Furthermore it is very difficult to find oscillatory free and stable solutions with the explicit time integration scheme unless extremely short time-steps are adopted. An unconditional implicit scheme is therefore used to avoid oscillations, and the method for tackling

the non-linearities is simply performed by searching for a time-step length where the solution is no longer significantly affected. It is realized that no guarantee that the 'true' solution can be followed in a non-linear problem by using successively shorter time steps since the implicit time integration is used.

It should be noted that a non-linearity is also introduced due to the existence of the product of the mass density of the fluid and its corresponding velocity. This is treated by letting one of the nodal parameters, for example the velocity, be a lumped element property and letting the other nodal parameter be descritizased in its normal way.

Another weakness in the proposed method is that linear approximations within the elements must be adopted for all three different unknown nodal parameters in order to justify the optimality of the Petrov-Galerkin method. This means that higher-order elements cannot be adopted for any of the three unknown nodal parameters without violating the arguments on which the Petrov-Galerkin weighting is based. Indeed, such combinations of different orders of approximations for different state variables have been shown to improve solutions in, for example, certain fluid dynamic problems.

The global equation system is non-symmetric, but this is a minor problem compared with the present convective terms and the non-linearities in the problem.

Here a simple one-dimensional problem will be considered only. The more general two- and three-dimensional cases can be obtained by generalization of the one-dimensional case to be presented. It should be observed, however, that bilinear elements are to be used when adopting the streamline Petrov-Galerkin method in two and three dimensions.

The whole global equation system, i.e. equations (15), (17) and (18), is arranged in the following standard manner

$$\mathbf{C}\dot{\mathbf{a}} + \mathbf{K}\mathbf{a} + \mathbf{f} = \bar{\mathbf{0}} \tag{19}$$

where $\mathbf{C}$ is the total damping matrix, $\mathbf{K}$ is the total 'stiffness', $\mathbf{f}$ contains information on both source terms and boundary conditions for the total equation system, the row vector $\mathbf{a}$ contains all three nodal parameters, i.e. the axial velocity of the fluid, the mass density of the fluid and the axial displacement of the solid. The property $\dot{\mathbf{a}}$ denotes the spatial time derivative of the corresponding nodal parameters.

The block matrixes within this system are established as

$$\begin{bmatrix} \mathbf{C}_u & \mathbf{0} & \mathbf{0} \\ \mathbf{0} & \mathbf{C}_\rho & \mathbf{0} \\ \mathbf{0} & \mathbf{0} & \mathbf{0} \end{bmatrix} \begin{bmatrix} \dot{\mathbf{a}}_u \\ \dot{\mathbf{a}}_\rho \\ \mathbf{0} \end{bmatrix} + \begin{bmatrix} \mathbf{K}_u & \mathbf{G}_{u\rho} & \mathbf{R}_{uw} \\ \mathbf{Q}_{\rho u} & \mathbf{K}_\rho & \mathbf{0} \\ \mathbf{H}_{wu} & \mathbf{Z}_{w\rho} & \mathbf{K}_w \end{bmatrix} \begin{bmatrix} \mathbf{a}_u \\ \mathbf{a}_\rho \\ \mathbf{a}_w \end{bmatrix} + \begin{bmatrix} \mathbf{f}_u \\ \mathbf{0} \\ \mathbf{f}_w^o \end{bmatrix} = \mathbf{0} \quad (20)$$

where the row-vectors $\mathbf{a}_u$, $\mathbf{a}_\rho$ and $\mathbf{a}_w$ denote the discrete values of the axial velocity of the fluid, the mass density concentration of the fluid and the axial displacement of the solid, respectively.

The Petrov-Galerkin weighting function v_u used in the determination of the axial velocity components of the fluid is given by (21a) and the approximation of the velocity at the nodes is given in (21b). That is,

$$v_u = \mathbf{c}^{\mathrm{T}} \left(\mathbf{N}_u^{\mathrm{T}} + \alpha_{opt.}^u \frac{h}{2} \frac{x_{1f}^{'}}{\left| x_{1f}^{'} \right|} \mathbf{B}_u^{\mathrm{T}} \right); \qquad x_{1f}^{'} = \mathbf{N}_u \mathbf{a}_u \quad (21)$$

where $\mathbf{c}^{\mathrm{T}}$ is an arbitrary matrix and where $\mathbf{N}_u$ is the one-dimensional linear shape function and $\mathbf{B}_u$ is the spatial derivative of $\mathbf{N}_u$. The optimality of the Petrov-Galerkin weighting is obtained by choosing the parameter $\alpha_{opt.}^u$ as

$$\alpha_{opt.}^u = \coth Pe^{eu} - \frac{1}{Pe^{eu}}; \qquad Pe^{eu} = \frac{\rho_f x_{1f}^{'} h}{2\mu_f} \quad (22)$$

where h denotes the element length and Pe^{eu} is the element Peclet number.

The weighting function v_ρ, to be used in the equation determining the mass density for the fluid, is in the same manner chosen as

$$v_\rho = \mathbf{c}^{\mathrm{T}} \left(\mathbf{N}_\rho^{\mathrm{T}} + \alpha_{opt.}^p \frac{h}{2} \frac{x_{1f}^{'}}{\left| x_{1f}^{'} \right|} \mathbf{B}_\rho^{\mathrm{T}} \right); \qquad \rho_f = \mathbf{N}_\rho \mathbf{a}_\rho \quad (23)$$

where the approximation of ρ_f is also shown. The parameter $\alpha_{opt.}^\rho$ is developed by the element Peclet number $Pe^{e\rho}$, in this case given as

$$\alpha_{opt.}^\rho = \coth Pe^{e\rho} - \frac{1}{Pe^{e\rho}}; \qquad Pe^{e\rho} = \frac{x_{1f}^{'} h}{2r} \quad (24)$$

where r is introduced for numerical convenience only. By setting r to a low numerical value (in this case the value $1e-25$ was adopted) the desired effect of introducing no 'diffusion' is obtained.

The standard procedure is adopted for the discretization of the axial displacement of the solid and in terms of the choice of weight function, i.e.

$$v_w = \mathbf{c}^{\mathrm{T}}\mathbf{N}_u^{\mathrm{T}}; \qquad w_1 = \mathbf{N}_w\mathbf{a}_w \tag{25}$$

By introducing a semi-discretization by using a weight function $W(t)$ in the time domain and then performing an integration between two time levels i and $i+1$ it can be established that only one parameter, denoted Θ, will determine the weighting method for equations containing first-order time derivatives. Hence, a transient solution procedure can be obtained in a straightforward manner. The parameter Θ is a number between 0 and 1 and is given as $\Theta = \frac{1}{\Delta t}\int_0^{\Delta t} W\tau d\tau / \int_0^{\Delta t} W d\tau$ where τ is a normalized time within the considered time step Δt. Different choices of the weight function $W(t)$ yield different values of Θ. The value $\Theta = 0$ is a truly explicit scheme and $\Theta = 1$ is a truly implicit scheme. The famous Crank-Nicholson scheme is obtained by setting $\Theta = 0.5$. The value $\Theta = 0.878$ is known as the Liniger algorithm, in which Θ is chosen to minimize the whole domain error for linear problems. The time discretizised version of (19) is

$$\mathbf{C}\left(\mathbf{a}_{i+1} - \mathbf{a}_i\right)/\Delta t + \mathbf{K}\left(\mathbf{a}_i + \Theta\left(\mathbf{a}_{i+1} - \mathbf{a}_i\right)\right) + \mathbf{f}_i + \Theta\left(\mathbf{f}_{i+1} - \mathbf{f}_i\right) = \mathbf{0} \tag{26}$$

where $\mathbf{a}_i$ is the known nodal parameter at the start of the time step and $\mathbf{a}_{i+1}$ is the unknown value searched for at the end at the time step Δt.

The different block matrixes in (20) will be explicitly shown below in their local element forms. The element shape functions $\mathbf{N}^e$ will be supplemented with a subscript u when associated with the axial velocity of the fluid and with a subscript ρ and w when associated with the mass density of the fluid and the axial displacement of the solid, respectively. The total equation system is obtained by a standard assembling procedure.

The local element damping matrix for the axial velocity equation is established as

$$\mathbf{C}_u^e = \int_0^h \left(\mathbf{N}_u^{e\mathrm{T}} + \alpha_{opt.}^u \frac{h}{2}\frac{x_{1f}'}{\left|x_{1f}'\right|}\mathbf{B}_u^{e\mathrm{T}}\right)\rho_f \mathbf{N}_u^e dx_1 \tag{27}$$

and the corresponding damping for the mass density equation for the fluid is given as

$$\mathbf{C}_\rho^e = \int_0^h \left(\mathbf{N}_\rho^{e\mathrm{T}} + \alpha_{opt.}^\rho \frac{h}{2}\frac{x_{1f}'}{\left|x_{1f}'\right|}\mathbf{B}_\rho^{e\mathrm{T}}\right)\mathbf{N}_\rho^e dx_1 \tag{28}$$

The 'stiffness' $\mathbf{K}_u$ is divided into three parts in its local element forms, i.e. $\mathbf{K}_u^e = \mathbf{K}_{u1}^e + \mathbf{K}_{u2}^e + \mathbf{K}_{u3}^e$, where $\mathbf{K}_{u1}^e$ is the standard 'stiffness', written as

$$\mathbf{K}_{u1}^e = \int_0^h \mathbf{B}_u^{e\mathrm{T}} 2\mu_f \mathbf{B}_u^e dx_1 \tag{29}$$

where is should be noted that the Petrov-Galerkin weighting reduces to the standard format. The second part of the 'stiffness' $\mathbf{K}_{u2}^e$ is due to the non-linear convective part in the equation determining the axial velocity of the fluid and is given as

$$\mathbf{K}_{u2}^e = \int_0^h \left(\mathbf{N}_u^{e\mathrm{T}} + \alpha_{opt.}^u \frac{h}{2} \frac{x_{1f}'}{|x_{1f}'|} \mathbf{B}_u^{e\mathrm{T}} \right) \rho_f x_{1f}' \mathbf{B}_u^e dx_1 \tag{30}$$

where the term $\rho_f x_{1f}'$ is treated as an element property which is lumped within each element. The last part involved in the local 'stiffness' $\mathbf{K}_{u3}^e$ is the contribution from the momentum supply 'force' which was assumed to be related to the fluid velocity through the material constant ξ_{fs}. $\mathbf{K}_{u3}^e$ takes the form

$$\mathbf{K}_{u3}^e = \int_0^h \left(\mathbf{N}_u^{e\mathrm{T}} + \alpha_{opt.}^u \frac{h}{2} \frac{x_{1f}'}{|x_{1f}'|} \mathbf{B}_u^{e\mathrm{T}} \right) \xi_{fs} \mathbf{N}_u^e dx_1 \tag{31}$$

The coupling term $\mathbf{G}_{u\rho}^e = \mathbf{G}_{u\rho 1}^e + \mathbf{G}_{u\rho 2}^e$ in its local element form is given as

$$\mathbf{G}_{u\rho 1}^e = -\int_0^h \left(\mathbf{N}_u^{e\mathrm{T}} + \alpha_{opt.}^u \frac{h}{2} \frac{x_{1f}'}{|x_{1f}'|} \mathbf{B}_u^{e\mathrm{T}} \right) \kappa_{fs} \mathbf{N}_\rho^e dx_1 \tag{32}$$

and

$$\mathbf{G}_{u\rho 2}^e = -\int_0^h \left(\mathbf{N}_u^{e\mathrm{T}} + \alpha_{opt.}^u \frac{h}{2} \frac{x_{1f}'}{|x_{1f}'|} \mathbf{B}_u^{e\mathrm{T}} \right) \vartheta_{fs} \mathbf{B}_\rho^e dx_1 \tag{33}$$

where the weighting function v_u is used together with a discretization of the mass density of the fluid as $\rho_f = \mathbf{N}_\rho \mathbf{a}_\rho$, and the gradient of ρ_f is given as $\mathbf{B}_\rho \mathbf{a}_\rho$ compare equation (23a) and (23b).

The coupling term modeling the effect of the trace of the strain tensor on the velocity of the fluid is in the studied one-dimensional case given as

$$\mathbf{R}_{uw}^e = -\int_0^h \left(\mathbf{N}_u^{e\mathrm{T}} + \alpha_{opt.}^u \frac{h}{2} \frac{x_{1f}'}{|x_{1f}'|} \mathbf{B}_u^{e\mathrm{T}} \right) \gamma_{fs} \mathbf{B}_w^e dx_1 \tag{34}$$

where it is noted that the axial displacement is approximated as $w_1 = \mathbf{N}_w \mathbf{a}_w$. The local element 'load' vector $\mathbf{f}_u^e$ contains the boundary conditions at the surface ds. The proper conditions at the boundary are a description of the thermodynamic pressure π_f^e and the mechanical traction t_{f1} in the fluid normal to the same surface, i.e.

$$\mathbf{f}_u^e = \int_{\partial s} \left(\mathbf{N}_u^{\mathrm{T}} + \alpha_{opt.}^u \frac{h}{2} \frac{x'_{1f}}{|x'_{1f}|} \mathbf{B}_u^{\mathrm{T}} \right) \left(-\pi_f^e + t_{f1} \right) ds \tag{35}$$

In the equation for the determination of the nodal values of the mass density of the fluid the term $-\rho_f \mathrm{div}\, \mathbf{x}'_f$ is present. In one dimension this term is formulated by the finite element approximations as

$$\mathbf{Q}_{\rho u}^e = - \int_0^h \left(\mathbf{N}_\rho^{e\mathrm{T}} + \alpha_{opt.}^\rho \frac{h}{2} \frac{x'_{1f}}{|x'_{1f}|} \mathbf{B}_\rho^{e\mathrm{T}} \right) \rho_f \mathbf{B}_u^e dx_1 \tag{36}$$

where ρ_f is treated as an element property which is lumped within each element. The 'stiffness' in the mass density equation for the fluid is divided into two parts, i.e. $\mathbf{K}_\rho^e = \mathbf{K}_{\rho 1}^e + \mathbf{K}_{\rho 2}^e$. The element 'stiffness' matrix $\mathbf{K}_{\rho 1}^e$ is introduced for numerical convenience only, as discussed above, by setting r to a low numerical value. $\mathbf{K}_{\rho 1}^e$ takes the form

$$\mathbf{K}_{\rho 1}^e = \int_0^h \left(\mathbf{B}_\rho^{e\mathrm{T}} \right) r \mathbf{B}_\rho^e dx_1 \tag{37}$$

The second part of the 'stiffness' $\mathbf{K}_\rho^e$ is due to the term $-\mathbf{x}'_f \cdot \mathrm{grad}\, \rho_f$ which is treated as a convective term in which the axial velocity of the fluid is introduced as a lumped element property. The gradient of ρ_f is discretized by the normal procedure. Hence, the one-dimensional case of $\mathbf{K}_{\rho 2}^e$ is

$$\mathbf{K}_{\rho 2}^e = \int_0^h \left(\mathbf{N}_\rho^{e\mathrm{T}} + \alpha_{opt.}^\rho \frac{h}{2} \frac{x'_{1f}}{|x'_{1f}|} \mathbf{B}_\rho^{e\mathrm{T}} \right) x'_{1f} \mathbf{B}_\rho^e dx_1 \tag{38}$$

The last row in the equation system (20) is the equation for the axial displacement of the solid in which the fluid is capillary sucked. In this equation row the standard Galerkin weighting will be adopted. The strains induced by the swelling of the solid due to the capillary sucked water will be calculated

by treating the term $\mathrm{div}\left(-\tau_f \Delta\rho_f \mathbf{I}\right)$ in the equation (17) as a 'pseudo load' within each element.

The stiffness takes the standard form

$$\mathbf{K}_w^e = \int_0^h \mathbf{B}_w^{e\mathrm{T}} k_s \mathbf{B}_w^e dx_1 \tag{39}$$

where $k_s = 2\left(\lambda_s + 2\mu_s\right)$ is a spring stiffness related to the elastic-modulus of the solid material. The momentum supply as constituted in (12) gives rise to the term

$$\mathbf{H}_{wu}^e = -\int_0^h \mathbf{N}_w^{e\mathrm{T}} \xi_{fs} \mathbf{N}_u^e dx_1 \tag{40}$$

And also the term

$$\mathbf{Z}_{w\rho}^e = -\int_0^h \mathbf{N}_w^{e\mathrm{T}} \vartheta_{fs} \mathbf{B}_\rho^e dx_1 \tag{41}$$

The local element load vector consists of two parts, i.e. $\mathbf{f}_w^{eo} = \mathbf{f}_{w1}^{eo} + \mathbf{f}_{w2}^e$. The row vector $\mathbf{f}_{w1}^{eo}$ is the pseudo-load induced by the swelling of the solid due to the presence of the fluid in the pore system. This term takes the local element form

$$\mathbf{f}_{w1}^{eo} = -\int_0^h \mathbf{B}_w^{e\mathrm{T}} \tau_s \Delta\rho_f dx_1 \tag{42}$$

where $\Delta\rho_f = \rho_f - \rho_f^+$ is considered as an element property.

The second part of $\mathbf{f}_w^{eo}$ is the boundary condition in terms of an applied mechanical traction normal to the boundary surface, i.e. $\mathbf{f}_{w2}^e$ is given as

$$\mathbf{f}_{w2}^e = -\int_{\partial s} \mathbf{N}_w^{e\mathrm{T}} t_{s1} ds \tag{43}$$

By standard assembling techniques the above local element matrixes are easily formulated at the global level. Hence, the equation system (20) is obtained.

6 Test results

Two test examples will be studied using the mixture theory and the numerical approach discussed in the previous section. Certain choices of the

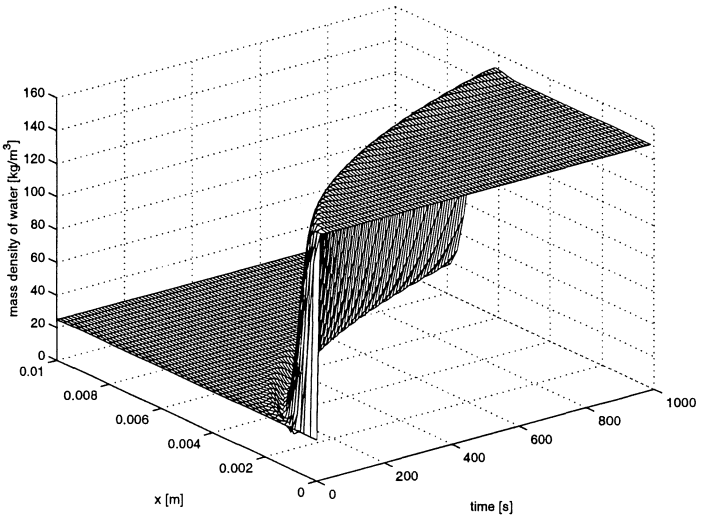

Figure 1: *Test example 1, calculated mass density concentration fields at different times from exposure.*

numerical values of the introduced material constants will be tested. The global response in terms of the weight change due to capillary suction will be compared to measured values obtained for concrete.

The first simulation is a case where water is exposed to a plane surface ($x = 0$)of a porous material. The 'active' mass density concentration of water in which all available porosity is filled with capillary sucked water is set to $\rho_f(0, t_o) = 150$ kg/m^3 and the initial condition is $\rho_f(x_1, t_o) = 25$ kg/m^3. The material coefficients used are: $\mu_f = 10^{-4}$ kg/s/m, which is 10% of the normal value of bulk water, and $\xi_{fs} = 0.1$ kg/s/m; all other coefficients are set to zero, in this the first example.

The boundary conditions used in equations (15) and (18) are based on the assumption that a time and length scale can be identified in which the mass concentration of water forms a discontinuous step where the velocity of the percolating water at the exposed surface is constant during an equivalent time step length $\Delta t_{equ.}$. The boundary condition to be used in (15) is then a description of the axial velocity of the water into the solid material surface during a time step length $\Delta t_{equ.}$. Simultaneously the boundary condition $\rho_f(0, t_o) = 150$ kg/m^3 is used in equation (18). In the subsequent time steps the velocity field is let die away by instead setting the thermodynamic

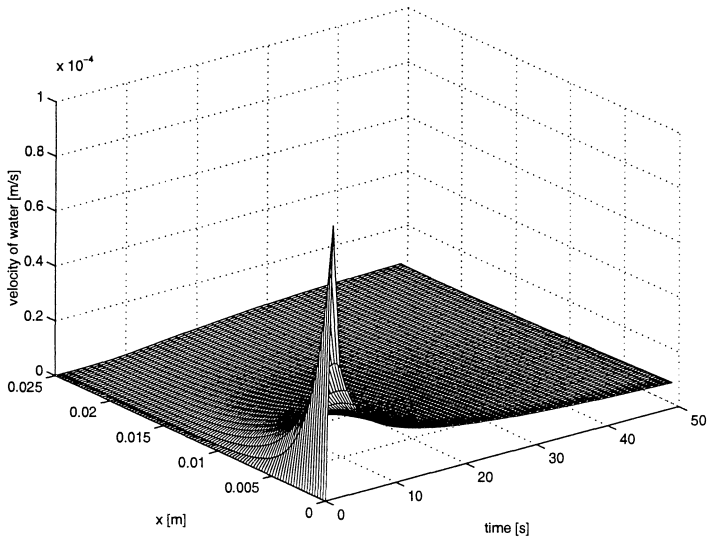

Figure 2: *Test example 1, calculated velocity fields at different times from exposure of water to a porous medium.*

pressure at the exposed boundary to zero. This choice can be justified by imagining that no curved liquid-air interfaces are present in the pore system near the exposed material surface when assuming that the whole active porosity is filled with capillary water instantaneously. External mechanical pressures or mechanical hydrostatic pressures are not considered in the test examples to be presented. The reason for not using a thermodynamic pressure at the boundary as the driving force for the studied capillary suction problem is that this pressure cannot be directly measured by laboratory experiments. The equivalent time step length $\Delta t_{equ.} = 1$ s is used, and the momentum pulse during this time step is set to $1.5 \cdot 10^{-2}$ kg/s/m^2. This smeared value corresponds to a velocity of water of 10^{-4} m/s and a mass density of 150 kg/m^3 at the boundary during the first second after exposure.

The result from the first test example is presented in Figure 1-3. In Figure 2 the computed velocity fields of the percolating fluid are presented at different times from exposure. It is seen that the axial velocity decays in the whole domain as the capillary suction proceeds. The corresponding mass density concentration fields are shown in Figure 1 and the global weight gain due to uptake of water in the porous material is shown in Figure 3 (dashed line). The global weight gain is also compared to the experimental obser-

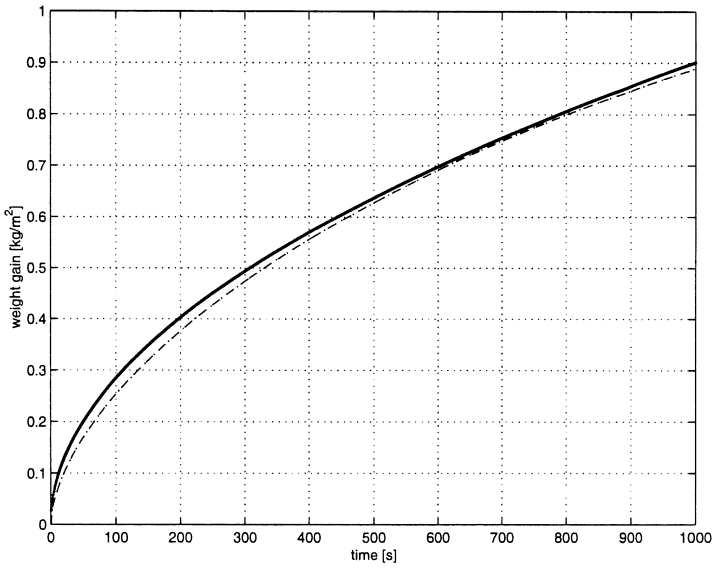

Figure 3: *Test example 1, comparison between calculated values (dashed line) and values given from the experimental evidence that for some materials the global weight gain due to capillary suction is linearly related to the square root of time (solid line). In this case with the factor* $k^{cap} = 0.0285\,\mathrm{kg/s^{1/2}/m^2}$.

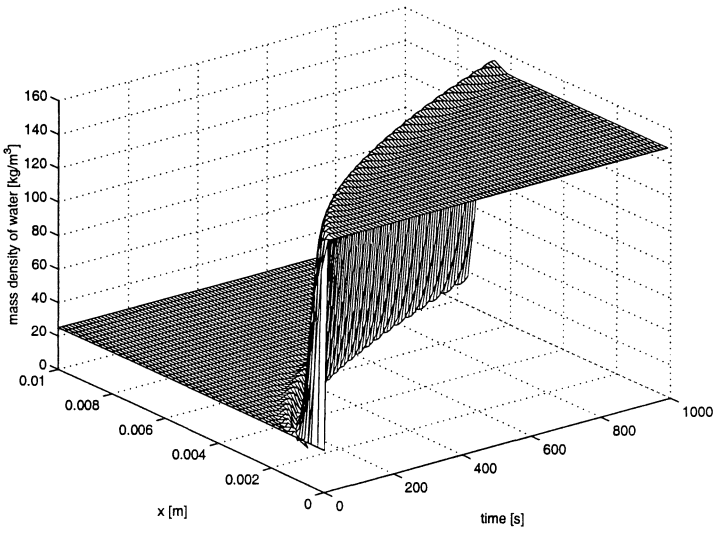

Figure 4: *Test example 2, mass density concentration fields of water in a porous material at different times from capillary suction exposure.*

vation that the global gain of mass of a capillary sucked sample is linearly related to the square root of time, see Figure 3 (solid line), ('time' is here referred to as the duration of the capillary suction process). The agreement between the simulation, using the above described material constants, and the square root dependent mass gain is fairly good, at least during the studied first 1000 seconds of exposure.

The value relating mass gain and the square root of time in Figure 3 is $k^{cap} = 0.0285\,\mathrm{kg/s^{1/2}/m^2}$. Experimental obtained values can, for example, be found in [10] and [11]. For well-cured concretes with water to cement ratios 0.5, 0.6 and 0.7 equilibrated in 50% relative humidity, the corresponding capillary suction numbers obtained were $k^{cap}_{0.5} = 0.013\,\mathrm{kg/s^{1/2}/m^2}$, $k^{cap}_{0.6} = 0.019\,\mathrm{kg/s^{1/2}/m^2}$ and $k^{cap}_{0.7} = 0.028\,\mathrm{kg/s^{1/2}/m^2}$. That is, the theoretical results obtained in test example 1 agree fairly well with the measured response for a concreted equilibrated at 50% relative humidity having a water cement ratio of 0.7. More experimentally obtained values of k^{cap} can be found in [12]. In [13] different values of k^{cap} and its dependence on the specimen's initial water content for sandstones are presented. Other test methods concerning capillary suction in porous materials can be found in, for example, [14] and [15].

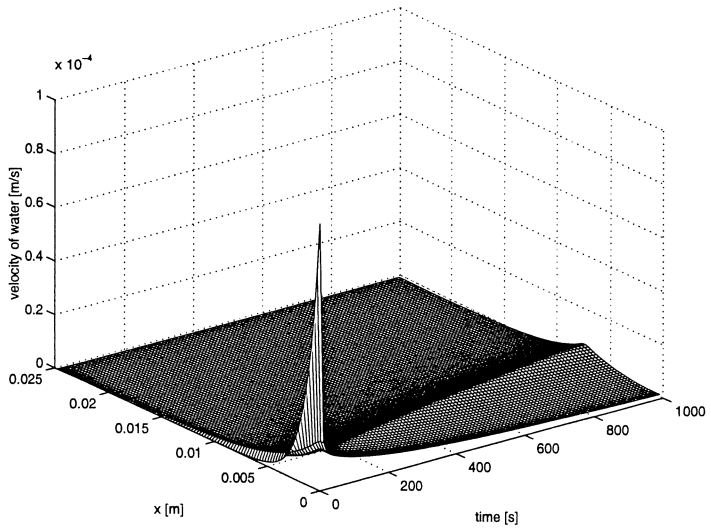

Figure 5: *Test example 2, velocity field at different times from capillary suction exposure.*

In the second test example the gradient of the mass density concentration will be included in the momentum supply term describing the interaction of 'forces' between the fluid and the solid, see equation (12). Furthermore, the axial stress due to swelling of the solid material will be computed with the proposed constitutive equation for the stress tensor for the solid, i.e. equation (13). The material coefficient relating the momentum supply to the mass density gradient is set to $\vartheta_{fs} = 2 \cdot 10^{-9}$ Nm/kg, and the axial elastic stiffness is set to $k = 30 \cdot 10^9$ N/m^2, and finally the stresses induced by moisture is calculated by using the coefficient $\tau_s = 0.2 \cdot 10^{-10}$ N/m^2/kg. The material coefficients used in test example 1 are also used in this the second example with the same numerical values. The same initial values and boundary conditions are also adopted in this second test example. Results are shown in Figures 4-6.

The velocity fields computed in test example 2 differ significantly from those obtained in the first example, compare Figure 2 and 5. The mass concentration fields obtained in example 2, see Figure 4, is somewhat more sharp in the propagating capillary 'front' compared to the first example. This effect is due to the inclusion of gradρ_f among the constitutive variables describing the momentum loss from the fluid to the solid pore walls.

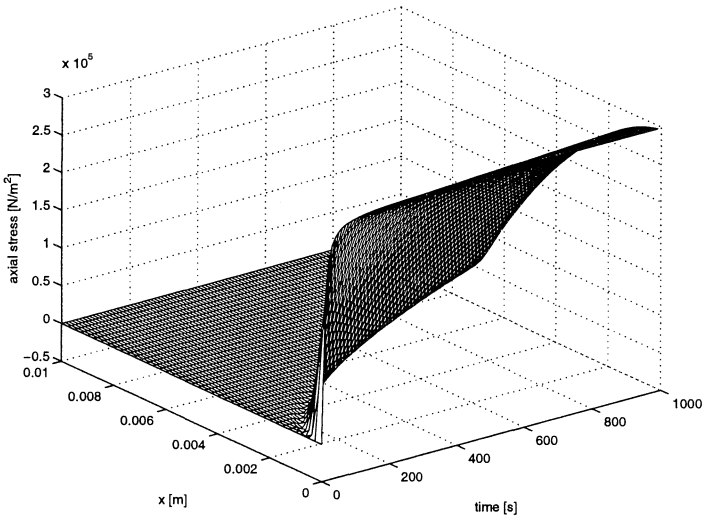

Figure 6: *Test example 2, axial stress due to swelling during the capillary suction process. The displacement of the specimen is set to zero at* $x = 0$.

7 Conclusions

It is possible to simulate the experimentally verified behavior of capillary suction by using the constitutive model described. It should be carefully observed, however, that the reliability of the adopted numerical approach has not been properly proven to converge towards true solutions. The approach was simply to use an Euler forward method for the non-linear element parameters together with the use of small time-steps.

Some difficulties were observed concerning the choice of boundary conditions in the momentum balance equation for the fluid, since a certain boundary value of the thermodynamic pressure cannot be justified by laboratory measurements in a simple manner. Instead a boundary condition in terms of a momentum pulse during an equivalent time-step was proposed. This condition seems somewhat easier to confirm with experiments.

The verified experimental behavior of a linear relationship between the global weight of sample plus capillary sucked water versus the square root of time was obtained in both test examples. This behavior is typical of less dense concrete and sandstones.

The inclusion of $\text{grad}\rho_f$ (test example 2) in the constitutive equation de-

scribing the momentum interaction between the fluid and the solid pore walls significantly changed the velocity fields at different times from exposure compared to the first test example. The calculated mass density concentration fields at different times from exposure do not, however, differ much from each other in the two studied examples.

The model accounts for stresses in the porous material induced by the presence of water in the pore system. The stresses in the porous material induced by the capillary suction flow of water are, however, very small compared to the stresses due to swelling of the solid in the proposed model.

The overall performance of the model indicates that it is a physically sound assumption to use the Navier-Posson law of a Newtonian fluid with a momentum source accounting for interaction with the pore walls when simulating capillary suction into porous materials.

An improvment of the model can consist of a more detailed study of the behavior at microscale together with upscaling techniques to the macroscale, for example, with the use of hybrid mixture theory where balance principles for the interfaces between solid-water, water-air and solid-air are also to be postulated.

References

[1] Bear, J. (1979). *Hydraulics of Groundwater*, McGraw-Hill, Inc. New York.

[2] Bowen, R. M. (1976). *Theory of Mixtures*, Part 1, in Continuum Physics, Edited by A. Cemal Erigen, Princeton University of Technology.

[3] Bennethum, L. S. and Cushman J. H. (1996). *Clarifying Mixture Theory and the Macroscale Chemical Potential for Porous Media*, International Journal of Engineering Science. Vol. 34, No. 14, pp. 1611-1621.

[4] Bennethum, L. S. and Giorgi T. (1997). *Generalized Forchheimer Equation for Two-Phase Flow Based on Hybrid Mixture Theory*, Transport in Porous Media. Vol. 26, No. 3, pp. 261-275.

[5] Achanta, S., Cushman J. H. and Okos M. R. (1994). *On Multicomponent, Multiphase Thermomechanics with Interfaces*, International Journal of Engineering Science. Vol. 32, No. 11, pp. 1717-1738.

[6] Johannesson, B. F. (1998). *Modelling of Transport Processes Involved in Service Life Prediction of Concrete, Important Principles*, Division of Building Technology, Lund University of Technology.

[7] Truesdell, C. (1985). *Rational Thermodynamics*, Second Edition. Springer-Verlag, New York.

[8] Zienkiewicz, O. C. and Taylor, R. L. (1989). *The Finite Element Method,* Fourth Edition, Vol. 2, McGraw-Hill, London.

[9] Bathe, K. J. (1996). *The Finite Element Procedures*, Prentice Hall, Englewood Cliffs, New Jersey.

[10] Fagerlund, G. (1980). Chapter 8. pp. 370 in *'Concrete Handbook'* (in Swedish).

[11] Fagerlund, G. (1982). *On the Capillarity of Concrete.* Nordic Concrete Research, Publication No. 1.

[12] Janz, M. and Johannesson, B. F. (1993). *A Study of Chloride Penetration into Concrete* (in Swedish), Division of Building Technology, Lund University of Technology.

[13] Janz, M. (1997). *Methods of Measuring the Moisture Diffusivity at High Moisture Levels*, Division of Building Technology, Lund University of Technology.

[14] Krus, M. (1995). *Moisture Transport and Storage Coefficients of Porous Mineral Building Materials, Theretical Principles and New Test Methods*, (in German), der Fakultät Bauingenieur- und Vermessungswesen der Universität Stuttgart.

[15] Pel, L. (1995). *Moisture Transport in Porous Building Materials*, Eindhoven University of Technology.